M. P. Sharma
Department of Petroleum Engineering,
University of Wyoming,
Laramie, Wy.

C. T. Crowe
Department of Mechanical Engineering,
Washington State University,
Pullman, Wash.

Application of Computer Modeling in the Design of a Multiphase Flow Metering System

Two numerical models (CONVAS and PSI-Cell) for analyzing steady non-equilibrium gas-particle flow through a venturi and an orifice plate are discussed. These models are validated by comparing the predictions with experimental data. Utilizing these models, parametric curves for venturis and orifice plates have been generated. Using these curves a methodology has been outlined for designing a two-phase mass flowmeter.

1 Introduction

The flow of gases with suspended particles is encountered in diverse industrially important energy and environment related applications. The applications range from pulverized coal combustion and gasification, air pollution control systems, pneumatic conveying of granular materials, and numerous chemical engineering processes to more exotic, advanced, and unconventional systems for nuclear, geothermal, and magneto-hydrodynamic power. These areas of application share a common need for improved measurement techniques, particularly flow metering. Unlike metering the flow of a single gaseous or liquid phase (for which accurate orifice and/or venturi coefficients are available), metering two-phase flows is more art than science. The complexity of multiphase flows has defied a systematic analytic design methodology.

Industrial methods for metering the flow of gas-particle suspensions currently in use are, by necessity, unsophisticated. For example, the flow rate of pulverized coal into a combustor is often metered by weighing the coal deposited on a moving belt. This system is not amenable to fine adjustments in the fuel flow rate to achieve the optimal combustion efficiency and economy. If a venturi or an orifice could be used on line with a certain level of reliability, a fuel-flow control system comparable to gas- or oil-fired burners could be realized. Similar situations arise in other industrial applications of gas-particle flows. Some attempts [1, 2] have been made to establish flow coefficients for gas-particle flow through orifices and venturis. Early studies [3] indicated that the presence of particles in a gas stream had no detectable effect on the pressure drop across an orifice; that is, the pressure drop across an orifice could be used to measure the gas flow rate even though particles were present in the gas stream. Further studies indicated that particles did affect the pressure drop across the venturi, the pressure drop being that corresponding to a homogenous gas-particle mixture. Thus the venturi measured the flow rate of the mixture. This observation was applied to the design of a flow-metering system consisting of an orifice and a venturi in series which yield data sufficient to determine the flow rate of each phase. Even though the device was successful on the laboratory scale, it was found inoperative on an industrial scale [4]. A re-evaluation of this technique shows that failure in industrial applications is attributable to unavailability of adequate scaling laws or analytical models to assess scale effects. These studies have shown that the effect of particles on the pressure drop across a venturi or orifice depends on the loading (mass of particles/mass of gas) and Stokes number [5].

The Stokes number is defined as the ratio of kinetic relaxation time of the particle to the system transit time. If the Stokes number is large, insufficient time is available for the particle to maintain velocity equilibrium with the gas and, correspondingly, there is little effect of the particles on the pressure field. Such is the situation for the orifice. On the other hand, if the system transit time is large compared to the particle's relaxation time, the particles are better able to maintain velocity equilibrium with the gas, and there is a corresponding effect on the pressure field. Such are the conditions for the venturi. At very large scale, the Stokes number is small for both the orifice and venturi, so the combination is incapable of detecting the flow rate of the individual phases. The limits of applicability can only be established by experiment or valid numerical models.

Gas particle flow through a venturi can be analyzed assuming quasi-one-dimensional flow using the "conservative variable" approach [6]. The acronym for this model is CONVAS (Conservative Variable and Source). A more sophisticated model—the PSI-Cell (Particle Source in Cell) [7]—is necessary for two dimensional orifice flow. The purpose of this paper is to illustrate the application of CONVAS and PSI-Cell models in the design of a venturi-orifice type two-phase flow meter. The viability of these models has been established by comparing the predictions with the experimental data.

2 Basic Approach

The primary difficulty is modeling two-phase flows arises

Contributed by the Fluids Engineering Division for publication in the JOURNAL OF FLUIDS ENGINEERING. Manuscript received by the Fluids Engineering Division January 16, 1987.

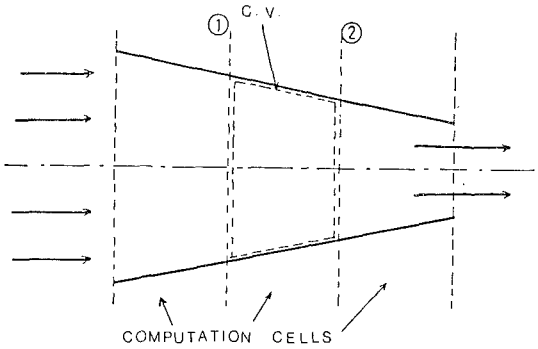

Fig. 1 Computational cells and control volume for CONVAS model

from the synergistic interaction of mass, momentum and energy transfer between the phases. This is called coupling phenomena [6].

The basic approach is first to divide the flow field into a series of computational cells and to regard each cell as a control volume. The change in the momentum of the particles as they pass through a cell is regarded as a source (or sink) to the momentum of the gaseous phase; that is, if a particle is accelerated by the flow field there must be a corresponding decrement of the gas momentum in the same direction within the cell.

The particle trajectories are obtained by integrating the equations of motion for the particles in the gas flow field, utilizing an appropriate expression for the drag coefficient. The particle trajectories and velocity along trajectories is obtained using the Lagrangian approach, which is the most straightforward approach for the particulate phase. Recording the momentum of the particles upon crossing cell boundaries provides the particle momentum source terms for the gas-flow equations.

3 CONVAS Model

The quasi one-dimensional gas-particle flow field is divided into a number of computational cells and each cell is considered a control volume, Fig. 1. The conservation equations for mass, momentum, and energy for a typical control volume can be written in terms of conservative variables X, Y, and A as:

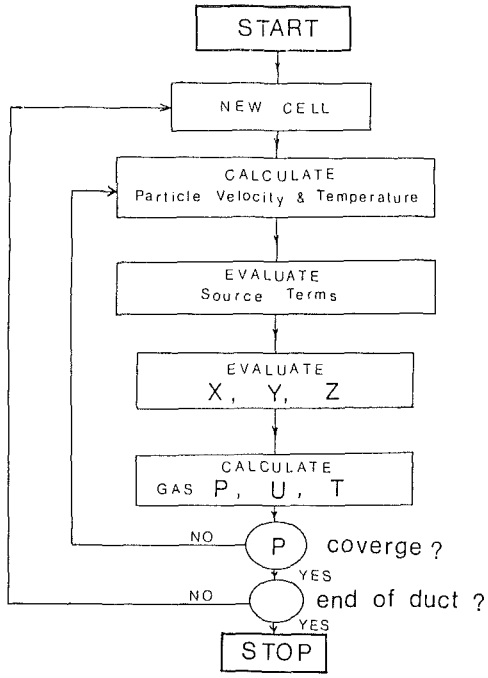

Fig. 2 Computational scheme for CONVAS model

$$X_2 = X_1 + \Delta \dot{m}_p \tag{1}$$

$$Y_2 = Y_1 + \Delta \dot{M}_P + \left(\frac{P_1 + P_2}{2}\right)(A_2 - A_1) - F_{wx} \tag{2}$$

$$Z_2 = Z_1 + \Delta \dot{E}_P + \dot{Q} \tag{3}$$

where the conservative variables are defined as:

$$X = \rho UA,\ Y = PA + XU,\ Z = (h + 1/2\ U^2)\rho UA \tag{4}$$

Nomenclature

A = area
A_p = particle cross section area
a = coefficients in momentum equations
C_D = drag coefficient
C_{pg} = specific heat of gas at constant pressure
C_v = specific heat of gas at constant volume
C_{pp} = specific heat of particle material
C_0, C_1, C_2, C = turbulence model coefficients
D = diameter of duct
d, d_p = diameter of a particle
d_0 = orifice diameter
d_t = throat diameter of a venturi
E = energy
$\Delta \dot{E}_P$ = energy source due to particles
F = force
F_{SL} = starting location mass-friction
F_{di} = particle size mass fraction
f = drag factor
G = mass flux, rate of turbulent kinetic energy generation
h = specific enthalpy
I = axial cell location
J = transverse cell location
k = specific heat ratio, kinetic turbulent energy
L = length of the converging section of a venturi
M = momentum flux
ΔM_A = momentum source due to area change
$\Delta \dot{M}_P$ = momentum source due to particles
m_p = mass of a particle
$\Delta \dot{m}_p$ = mass source term
$\dot{m}_p$ = mass flow rate of particles
$\dot{m}_g$ = mass flow rate of gas
n = number of particles/time
P, p = pressure
$\Delta P_{mt}, \Delta P_{mo}$ = pressure drop for mixture flow in venturi (throat); in orifice
$\Delta P_{gt}, \Delta P_{go}$ = pressure drop for gas flow in venturi (throat); in orifice
$\dot{Q}$ = heat transfer rate
R = gas constant
Re = particle Reynolds number
S = source term
St = Stokes number
St_o = Stokes number for orifice
St_v = Stokes number for venturi

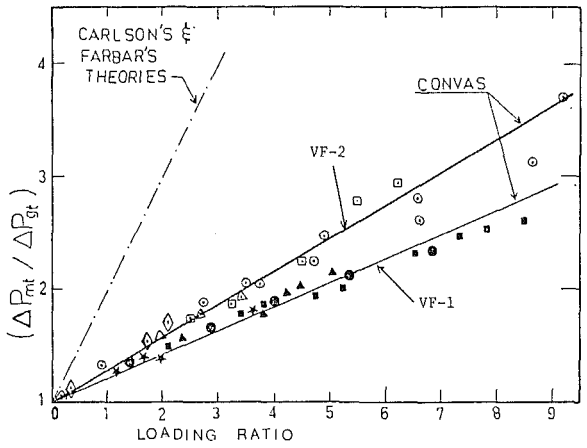

Fig. 3 Comparison of CONVAS predictions with Farber's experimental data [1] for two venturis VF-1 and VF-2

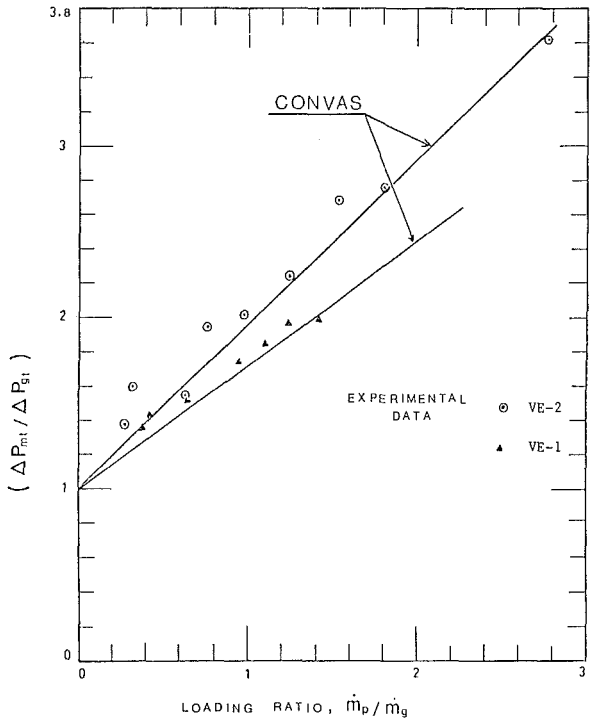

Fig. 4 Comparison of CONVAS predictions and Sharmas' experimental data for two venturi's VE-1 and VE-2 [5]

$\Delta\dot{m}_p$, $\Delta\dot{M}_p$, and $\Delta\dot{E}_P$ are source terms due to particles. h, P, ρ, U are specific enthalpy, pressure, density, velocity of gas and A is cross-sectional area of the duct. F_{wx} and $\dot{Q}$ are shear force and heat transfer at the wall of the duct.

The source terms are evaluated by integrating the equations of motion and energy of a particle moving in a gas medium. The reader should refer to the reference (7) for details.

$$\Delta\dot{M}_p = z\,\dot{m}_g\,(V_1 - V_2) \tag{5}$$

$$\Delta\dot{E}_p = \tfrac{1}{2} z\,\dot{m}_g\,(V_1^2 - V_2^2) + z\,\dot{m}_g C_{pp}\,(T_{p1} - T_{p2}) \tag{6}$$

The solution procedure starts by guessing P_2 and then following calculational steps shown on the flow chart, Fig. 2.

To illustrate the applicability and reliability of CONVAS, the predictions of the nondimensional pressure differential through a venturi are compared with the experimental data of Farbar [2] (coal particles), and Sharma [5] (silica particles), Figs. 3 and 4. In these figures the results predicted by CONVAS-theory (the solid lines) are compared with the experimental data (dots) obtained by Farber [1] (in Fig. 3) and Sharma [5] (in Fig. 4). Two lines in Fig. 3 belong to two different designs of venturis, used by Farber. Similarly in Fig. 4, the two lines belong to the results of two different designs. Details of these designs are available in reference [5].

The excellent agreement establishes that CONVAS can be reliably used in the design and analysis of gas-particle flows through venturis.

Nomenclature (cont.)

T = temperature of gas
T_p = particle temperature
t = time
T_g = relaxation time for gas flow field
U = x-direction velocity of the gas (one dimensional)
$\mathbf{u}$ = gas velocity vector
$\mathbf{u}_p$ = velocity vector for a particle
V = particle velocity (one dimensional)
X = mass conservative variable
x = first coordinate direction
Y = momentum conservative variable
y = second coordinate direction
Z = energy conservative variable
z = particle loading ratio
β = diameter ratio ($d/_0D$ for orifice, d_t/D for venturi
θ = angle of converging section of venturi
ϵ = turbulent energy dissipation
σ_κ, σ_ϵ = turbulent Prandtl numbers for κ and ϵ, respectively
ρ = density of gas
ρ_p = density of particle material
τ = dynamic characteristic time
τ_Q = thermal characteristic time
μ = viscosity, microns
ν = kinematic viscosity
κ = turbulent kinetic energy

Subscripts

1 = upstream conditions
2 = downstream conditions
I, J = index for grid nodes
N, S, E, W = north, south, east, west
o = orifice
g = gas
v = venturi
m = mixture of gas and particles

Superscripts

j = trajectories
x = axial direction
y = traverse direction

Acronyms

CONVAS = conservative variable and source model
PSI-Cell = particle-source-in-cell model
SM = signal Magnification

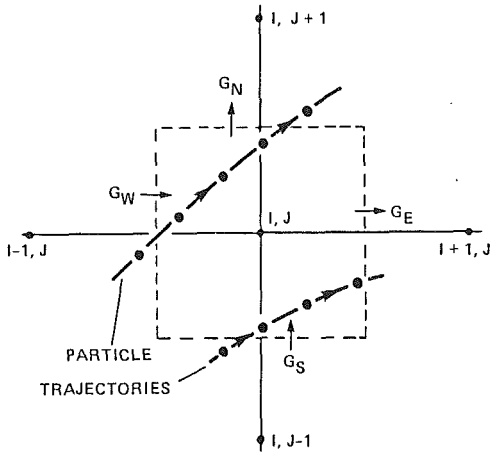

Fig. 5 Computational cell for PSI-cell model

4 PSI-Cell Model

The two-dimensional steady flow of gas-particle mixture through an orifice can be analyzed using the PSI-Cell Model [5]. After dividing the flow field into a number of rectangular cells, finite-difference equations for momentum of the gas phase are written for each cell, incorporating the contribution due to the condensed phase as a source term. The entire flow-field solution is obtained by solving the system of algebraic equations constituting the finite-difference equations for each cell.

Refer to the cell shown in Fig. 5 which encloses a typical node (I, J). The four faces of this cell are identified as points on a compass: north, south, east, and west. The continuity equation for steady flow of the gas-particle mixture through this cell (control volume) is:

$$G_E + G_N - G_W - G_S + \Delta\dot{m}_p = 0 \tag{7}$$

where G_i is the mass flux rate of the gas through the "ith" face and $\Delta\dot{m}_p$ is the net mass efflux rate of the particles from the cell.

If the particles are not reacting (burning, evaporating, or condensing), then the mass source term is zero. Such is the situation for the application of this paper.

Having located the cells for the continuity equation as enclosing the nodal points, the cells for the momentum equation must be located between nodes. Referring to Fig. 5, one notes that the u-component of velocity in the continuity equation is not the velocity at the nodal point but halfway between nodes. Consequently, the control volume used to solve for u from the x-momentum equation is displaced from that used for the continuity equation. The momentum equation in the x-direction for steady flow requires that

$$-M_W^x + M_E^x - M_S^x + M_N^x + \Delta M_P^x = (P_{I-1,J} - P_{I,J})A_N + S_P^x \tag{8}$$

where M_P^x is the momentum flux of the gas in the x-direction across the "ith" face, ΔM_P^x is the net efflux of x-momentum from the cell due to the droplets, $P_{I,J}$ is the pressure at node (I,J), and S_P^x arises from the variation in effective viscosity in the flow field [8]. The momentum flux consists of that due to convection and diffusion (viscosity). Body force terms have been neglected.

One notes that the net efflux of momentum due to the droplets can be regarded as the momentum source term to the gaseous phase. The net droplet momentum efflux from a cell due to trajectory "j" which traverses the cell is given by

$$\Delta\mathbf{M}_{P,j} = \dot{n}_j[(m\mathbf{V})_{\text{out}} - (m\mathbf{V})_{\text{in}}] \tag{9}$$

where $\mathbf{V}$ is the droplet velocity. The net momentum efflux for all trajectories which pass through the cell is

$$\Delta\mathbf{M}_P = \sum_j \Delta\mathbf{M}_{P,j} \tag{10}$$

The cell used for the y-momentum equation is located below and midway between the nodes (I,J) and (I,$J-1$).

Two more equations are used in the numerical program to model the turbulence and to determine the effective viscosity. The turbulent field is described by the local intensity of turbulence and the dissipation rate, commonly referred to as the k-ϵ model.

In order to evaluate the source terms due to the presence of the particles, the particle equation of motion is integrated utilizing the velocity and pressure field of the gas. The original details are available in reference [7]. The rearranged form of the equation of motion of a particle is

$$d\mathbf{V}/dt = (18\mu f/\rho_p d^2)(\mathbf{U} - \mathbf{V}) \tag{11}$$

where, $f = C_D\ \text{Re}/24 = 1 + 0.15\ \text{R}_e^{.687}$ for $\text{Re} \le 1000$

$$\text{Re} = \frac{\rho\,|\mathbf{V} - \mathbf{V}|\,d}{\mu} = \text{particle Reynolds number}$$

It is to be noted that the Reynolds number used in equation (11) is particle Reynolds number (not pipe Reynolds number) and is defined in a special way. Particle drag coefficient correlation given above has been found valid up to particle Reynolds number value of 1000. The critical value of particle Reynolds number (at which laminar to turbulent transition would occur) is approximately 1.0.

Integrating equation (11) assuming the gas velocity is constant over the time of integration yields

$$\mathbf{V} = \mathbf{U} - (\mathbf{U} - \mathbf{V}_0)\exp(-\Delta t/\rho_P d^2/18\mu f) \tag{12}$$

where V_0 is the initial particle velocity and Δt is the time interval. After determining the new droplet velocity after time Δt, the new droplet location is determined from

$$\mathbf{x}_p = \mathbf{x}_{p,o} + (\mathbf{V} + \mathbf{V}_o)\Delta t/2 \tag{13}$$

where $\mathbf{x}_{p,o}$ is the droplet position at the beginning of the time increment.

Turbulence Model Equations. The turbulence closure problem has to be solved before attempting to solve the conservation of mass and momentum equations. A summary of the existing turbulent closure models has been compiled by Launder and Spalding [9]. A two equation model is used in this analysis to account for the turbulence and to determine the effective viscosity. The turbulence field is described by the local kinetic energy (intensity) of turbulence (κ) and the dissipation rate (ϵ). The two-equation model consists of the solutions to the transport equations for these two physical quantities κ and ϵ.

$$\frac{\partial}{\partial x}(\rho u\kappa) + \frac{\partial}{\partial y}(\rho v\kappa) - \frac{\partial}{\partial x}\left(\frac{\mu}{\sigma_\kappa}\frac{\partial \kappa}{\partial x}\right) - \frac{\partial}{\partial y}\left(\frac{\mu}{\sigma_\kappa}\frac{\partial \kappa}{\partial y}\right) = G - C_0\rho\epsilon \tag{14}$$

$$\frac{\partial}{\partial x}(\rho u\epsilon) + \frac{\partial}{\partial y}(\rho v\epsilon) - \frac{\partial}{\partial x}\left(\frac{\mu}{\sigma_\epsilon}\frac{\partial \epsilon}{\partial x}\right) - \frac{\partial}{\partial y}\left(\frac{\mu}{\sigma_\epsilon}\frac{\partial \epsilon}{\partial x}\right) = \frac{C_1\epsilon G}{\kappa} - \frac{C_2\rho\epsilon^2}{\kappa} \tag{15}$$

$$G \equiv 2\mu\left[\left(\frac{\partial u}{\partial x}\right)^2 + \left(\frac{\partial v}{\partial y}\right)^2\right] + \mu\left[\frac{\partial u}{\partial y} + \frac{\partial v}{\partial x}\right]^2$$

where σ_κ and σ_ϵ is considered as the turbulent Prandtl numbers for κ and ϵ, and are treated as constants. C_0, C_1, and C_2 are other constants. G is rate of generation of κ and $\rho\epsilon$ is rate of

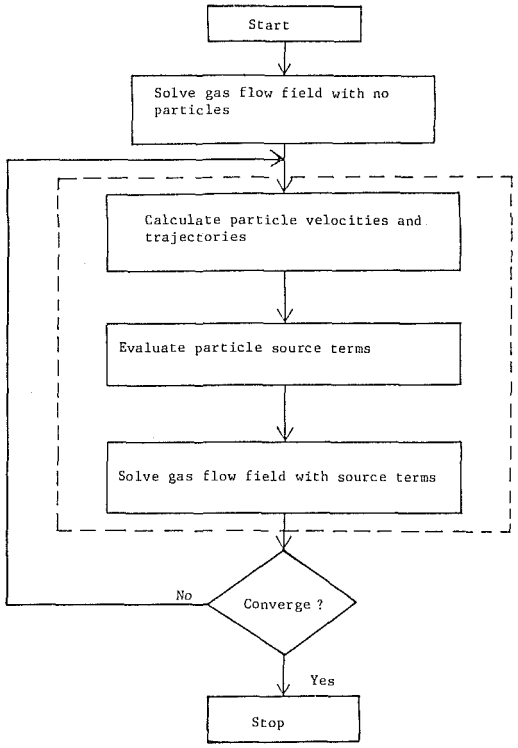

Fig. 6 Computational scheme for PSI-cell model

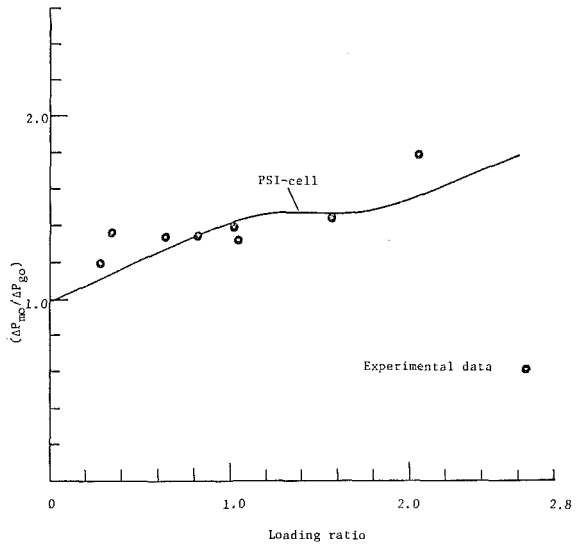

Fig. 7 Comparison of PSI-cell predictions and experimental data for orifice flow [5]

dissipation. The finite-difference form of these equations is incorporated into the program to yield the kinetic energy of turbulence and the dissipation rate as related to the mean velocity field. Having evaluated the turbulence intensity and dissipation rate in a cell, the effective viscosity is determined using Prandtl-Kolmogorov formula:

$$\mu = \frac{C_\mu \rho \kappa^2}{\epsilon} \tag{16}$$

where C_μ is a constant.

The values of various global constants in this model are taken from [9].

No attempt is made to include the effect of particles on the turbulence field because little is known about the quantitative effect of particle size and concentration on the turbulence parameters.

It should be also noted that though the κ-ϵ model is a significant improvement over mixing length models, it still assumes that Reynolds stresses depend only on the local mean velocity gradients, and that turbulence adjusts itself instantly to local changes in the mean flow field. On the contrary, it is well established that "history" and "action-at-distance" are dominant in establishing local turbulence characteristics. Two-equation model, however, has been found satisfactory in many flows of interest [9].

The complete solution for the droplet-gas flow field is executed as shown in Fig. 6. The calculation is done by first solving the gas flow field assuming no droplets are present. Using this flow field, droplet trajectories are calculated, and the momentum source terms for each cell throughout the flow field are determined. The gas flow field is solved again incorporating these source terms. The new gas flow field is used to establish new droplet trajectories which constitutes the effect of the gas phase on the droplets. Calculating new source terms and incorporating them into the gas flow field constitutes the effect of the droplet cloud on the gas phase, thereby completing the "two-way" coupling. After several iterations the flow field equations are satisfied to within a predetermined value and the solution which accounts for the mutual interaction of the droplets and gas is obtained.

The comparison of the predicted and measured pressure drops across an orifice is shown in Fig. 7. The data are plotted as the ratio of pressure drop with particles to that for a clean gas versus the loading ratio (mass flow rate of particles/mass flow rate of gas). By definition, the pressure ratio is unity at a loading ratio of zero. The data were taken from [5]. One notes favorable agreement between the predicted and measured values, which lends support to the validity of the model. The validation of these models have been further established in other gas-particle flow applications and are reported in a recent review paper [10].

5 Design Curves

CONVAS and PSI-Cell models are used to generate design curves for designing a two-phase flowmeter consisting of a venturi and an orifice place. The primary design parameters are,

$$\mathrm{St}_v = \frac{\rho_p d^2{}_p}{18 \cdot \mu \cdot f} \cdot \frac{U_{\text{in}}}{L} \cdot \frac{D - d_t}{2L} \quad \text{(for venturi)} \tag{17}$$

$$\mathrm{St}_o = \frac{\rho_p d^2{}_p}{18 \cdot \mu \cdot f} \cdot \frac{U_{\text{in}}}{D} \quad \text{(for orifice)} \tag{18}$$

$$\beta = d_o/D \text{ (orifice)}; = \frac{d_t}{D} \quad \text{(venturi)} \tag{19}$$

$$Z = m_p/m_g \tag{20}$$

$$\theta = \frac{D - d_t}{2L} \tag{21}$$

where D is diameter of duct, d is diameter of orifice, d_t is venturi throat diameter, and L is length of converging section of venturi.

The design curves for orifice plate are shown in Fig. 8. It shows the variation of the threshold values of particle loading (z) with Stokes number (St_o) for different β values (d_o/D). The threshold value of loading is defined as the maximum value of z for which particles have "no effect" on the gas pressure field (for a given St_o and β). Each curve divides the z-St_o plane into two regions. Left of this curve is the region of "no effect" of particles on the gas pressure field. To measure the gas flow rate only, an orifice has to be designed such that the parameters lie in the "no effect" region of this plane.

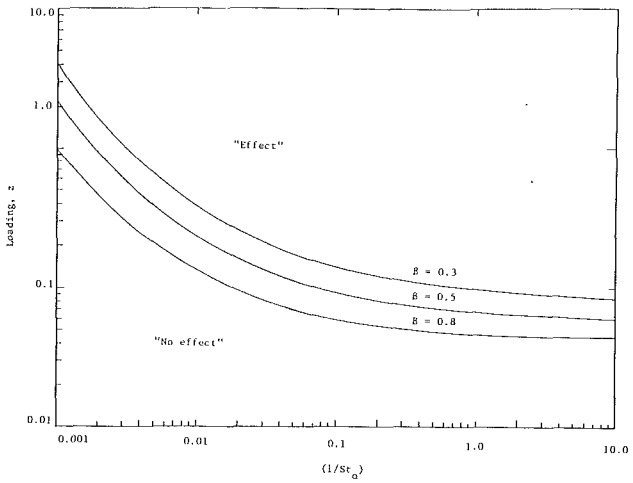

Fig. 8 Design curves for orifice plates

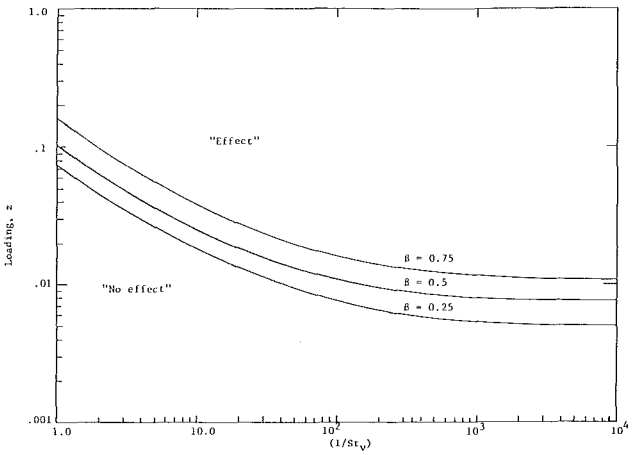

Fig. 9 Design curves for venturis

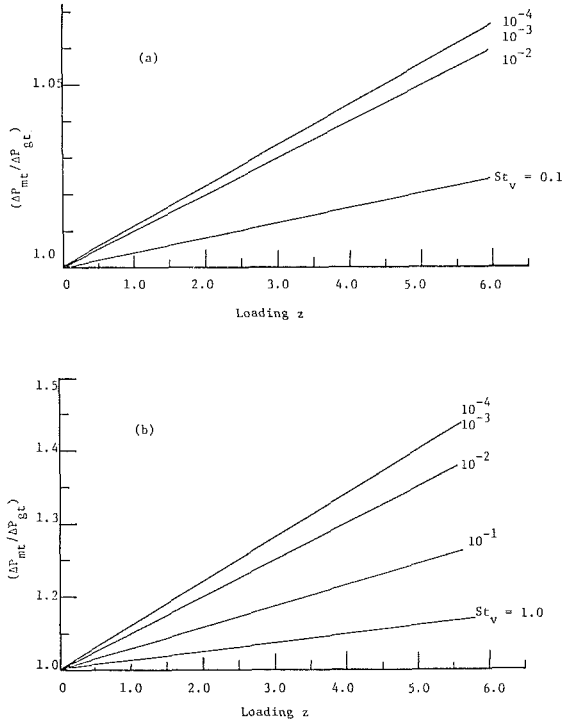

Fig. 10 Signal magnification curves

The design curves for venturis are shown in Figs. 9 and 10. Figure 9 shows the variation of the threshold values of particle loading (z) with the Stokes number (St_v) for different β values (d_t/D). Each curve divides the plane into regions of "no effect" and "effect" of particles on the venturi throat pressure. To be able to measure the particle flow rate, the venturi must be designed such that the parameters lie in the "effect" region of the curve.

Figure 10 is a plot of signal magnification ($SM = \Delta P_{mt}/\Delta P_{gt}$) versus the particle loading for different values of venturi Stokes number (St_v). ΔP_{mt} and ΔP_{gt} are pressures at the venturi throat for mixture and gas flow, respectively. Using the SM curves, a venturi can be designed to produce a desired magnification (for accuracy of measurement) of particle effect on the throat pressure drop. The SM curves can also be used to calculate particle loading if gas flow rate is known and ΔP_{mt} is measured.

6 Design Methodology

Given the information on the range of fluid flow rates, fluid properties, particle material density and size distribution, range of particle loading and signal magnification requirements, following steps should be followed in designing a flowmeter:

1. Calculate St_o based on the smallest size of the particle in the flow.

2. Determine a value of β for the maximum value of particle loading using Fig. 8, such that there is no effect of the particles on the orifice pressure drop.

3. Calculate τ_p based on the largest size of the particle in the flow and then follow either one of the following steps:

(a) For the minimum value of particle loading, choose a combination of β and St_v from Fig. 9 such that the particles have an effect on the venturi throat pressure. From this value of St_v and calculated value of τ_p, determine an appropriate value of L (or θ) using equation (14).

(b) If a requirement on the signal magnification is to be met, Fig. 10 should be used. For the given value of minimum loading and signal magnification, choose a combination of β and St_v from Fig. 10. Using equation (14) and the value of ρ_p from Step 3, determine an appropriate value of L (or θ) for the venturi.

The two primary elements should be separated by a minimum distance of ten pipe diameters. Taps should be made according to standard design specifications [11].

Design curves in Figs. 8 to 10 have been generated for a Reynolds number (Re) range around 10,000. For Re vastly different than this value, new sets of design curves should be generated using the computer programs discussed in previous sections and available in [5].

The venturi can be installed upstream or downstream of the orifice. There is no theory to establish the preference of one choice over the other. For a compact flowmeter, the venturi should be placed on the upstream side so that a minimum flow disturbance is created before the orifice plate, and, therefore, the distance between the two elements could be kept to minimum. This arrangement has been favored in practice.

7 Conclusions

A philosophy and methodology of design for a gas-particle flowmeter using orifice plate and venturi elements has been presented. The methodology is based upon newly developed theoretical models and methods of calculating gas-particle flows. These theoretical models have been validated with experimental data for dilute gas-particle flows.

This paper has presented a conceptual design of a flow meter for multiphase flow environment. The questions related to performance and accuracy of such a flowmeter are matters

of actual experience in installation, operation and extensive experimentation. This is another phase of this problem. This study sets the theoretical basis for such investigations.

Acknowledgments

The authors acknowledge the invaluable assistance of Linda Brooks of the University of Wyoming in typing the manuscript. The valuable assistance of Mr. Haus Hauge and Mr. Trond Jensen, graduate students of Petroleum Engineering, University of Wyoming, in typing the complicated equations has left marks of their newly acquired expertise and is sincerely appreciated.

References

1 Farbar, L., "The Venturi as a Meter for Gas-Solids Mixtures," *Ind. Eng. Chem.*, Vol. 44, 1952, p. 2947.

2 Graczyk, C., "The Application of the Venturi Tube to the Measurement Rate of Coal Dust Flow Transported by Air," *Acta. Imeko*, Vol. 4, 1961, p. 251.

3 Carlson, H. M., Frazier, P. M., and Engdahl, R. B., "Meter for Flowing Mixtures of Air and Pulverized Coal," *Trans. ASME*, Vol. 70, 1948, p. 65.

4 Saltsman, R. D., "The BCR Gas-Solids Flow Meter," Inf. Cir. 8314, U.S. Bureau of Mines, 1966.

5 Sharma, M. P., "Numerical and Experimental Study of Gas-Particle Flows in Orifices and Venturis: Application to Flow Meter Design," Ph.D. thesis, Washington State University, 1977.

6 Sharma, M. P., and Crowe, C. T., "A Novel Physico-Computational Model for Quasi-One-Dimensional Gas-Particle Flows," ASME JOURNAL OF FLUIDS ENGINEERING, Vol. 100, Sept. 1978.

7 Crowe, C. T., Sharma, M. P., and Stock, D. E., "The Particle-Source-in-Cell (PSI-Cell) Model for Gas-Droplet Flows," ASME JOURNAL OF FLUIDS ENGINEERING, Vol. 99, June 1977.

8 Wormeck, J. J., "Computer Modeling of Turbulent Combustion in a Lonwell Jet-Stirred Reactor," Ph.D. thesis, Washington State University, 1976.

9 Launder, B. E., and Spalding, D. B., *Mathematical Models of Turbulence*, Academic Press, New York, 1972.

10 Crowe, C. T., "Review of Numerical Models for Dilute Gas-Particle Flows," ASME JOURNAL OF FLUIDS ENGINEERING, Vol. 104, Sept. 1982.

11 Bean, H. S., *Fluid Meters—Their Theory and Applications*, 6th ed. ASME, New York, 1971.